УДК 551.243 (51)
https://doi.org/10.26516/2541-9641.2023.1.52

Этапы подготовки к прерывистому скольжению на предварительно вырезанных разломах в лабораторных моделях и проверка этапов в природе

С.А. Борняков[a], Я. Го[b], И.А. Пантелеев[c], Я-К Жуо[b], А.А. Добрынина[a], В.А. Саньков[a,d], Д.В. Салко[a], А.Н. Шагун[a], А.А. Каримова[a,d]

[a]*Институт земной коры СО РАН, г. Иркутск, 664033, Россия*
[b]*Институт геологии, Сейсмологического бюро Китая, г. Пекин, Китай*
[c]*Институт механики сплошных сред УрО РАН, г. Пермь, Россия*
[d]*Иркутский государственный университет, г. Иркутск, Россия*

Аннотация. Исследование посвящено аналоговому моделированию процесса прерывистого скольжения (“stick-slip”) вдоль существующего крупного разлома в упруго-вязкопластической модели при постоянной скорости деформации. Основываясь на полученных результатах и данных в публикациях (Ma et al., 2012, 2014), мы выделяем стабильную, метастабильную и метанестабильную стадии процесса подготовки динамической подвижки по модельному разлому. Выполненные эксперименты показали, что активизация разлома обеспечивается механизмом сегментации. Приводится анализ характера сегментации в пределах одного акта активизации разлома. Показано, что процесс сегментации реализуется в рамках регрессивного и прогрессивного сценариев. Регрессивная сегментация происходит на стабильных и метастабильных стадиях деформационного процесса. При регрессивной сегментации уменьшается количество активных сегментов и их длина. Прогрессивная сегментация начинается на ранней подстадии метанестабильной стадии процесса скольжения и диагонстируется по увеличению активных сегментов до некоторого критического уровня. На поздней подстадии этой стадии просиходит быстрое разрастание и объединение всех сегментов с последующей полной активизацией всего разлома.

Результаты моделирования использованы для интерпретации данных мониторинга деформаций горных пород на геодинамическом полигоне перед Быстринским землетрясением. Проведенный анализ подтверждает, что специфические особенности аномальной деформации пород аналогичны деформационным признакам, наблюдаемым вдоль модельного разлома на метанестабильной стадии. Это позволяет предполагать, что метанестабильное состояние разлома может быть использовано в качестве краткосрочного предвестника землетрясений.

***Ключевые слова**: аналоговое моделирование, прерывистое скольжение, разлом, сегментация, метанестабильная стадия, землетрясение, предвестник.*

Stages of Stick-Slip Preparation on Precut Faults in Laboratory Models and Verification of the Stages in Nature

S.A. Bornyakov[a], Y. Guo[b], I.A. Panteleev[c], Y-Q Zhuo[b], A.A. Dobrynina[a], V.A. Sankov[a,d], D.V. Salko[a], A.N. Shagun[a], A.A. Karimova[a,d]

[a]*Institute of the Earth’s Crust, Siberian Branch of the Russian Academy of Sciences, Irkutsk, 664033, Russia*
[b]*Institute of Geology, China Earthquake Administration, Beijing, China*
[c]*Institute of Continuous Media Mechanics, Ural Branch of the Russian Academy of Sciences, Perm, Russia*
[d]*Irkutsk State University, Irkutsk, Russia*

Abstract. This study is focused on analog modeling of the stick-slip process along an existing large fault in an elastic-viscoplastic model subjected to loading at a constant strain rate. Based on our model results and data from (Ma et al., 2012, 2014), we distinguish stable, meta-stable, and meta-instable stages of the stick-slip process (the latter includes the early and late sub-stages). Our experiments show that the fault is periodically reactivated by segmentation. We analysed this mechanism from one fault reactivation to another, and identified regressive and progressive trends of segmentation. The regressive segmentation takes place during the stable and meta-stable stages of the stick-slip process. Under regressive segmentation the number of active segments and their lengths are reduced. The progressive segmentation is initiated at the early meta-instable sub-stage of the stick-slip process. Its activity is desplayed by an increase in the number of active segments to a certain critical density, while their pattern becomes more chaotic. In the late sub-stage, number of segments decreases as they rapidly grow and join with each other to form larger active segments, up to full reactivation of the entire fault.

For comparison with the model results, we interpret rock deformation monitoring records before the Bystroe earthquake. Our analysis confirms specific features of the anomalous rock deformation that are similar to the strain features observed along the model fault during the meta-instable stage. There are evidence to suggest that meta-instability of a fault is a potential candidate to short-term precursor of earthquakes.

Keywords*: analogue modeling, stick-slip, fault, segmentation, meta-instable stage, earthquake, precursor.*

Introduction

In recent studies, tectonic earthquakes are generally related to two well-known seismic source mechanisms based on avalanche unstable fracturing (AUF) and stick-slip models. In AUF models, several short fractures rapidly join together to make a long fault, and their linkage is followed by a seismogenic displacement (Myachkin, 1978). In stick-slip models, seismogenic displacements take place along an existing fault during its reactivation (Brace and Byerlee, 1966). It is widely accepted that the stick-slip mechanism is a principal pattern of fault reactivation and a possible mechanism for earthquake occurrence at large faults located in seismically active zones of the continental lithosphere. Physical models and numerical simulations of the stick-slip mechanism have joined the forefront of investigations aimed at earthquake prediction. They aim to assess the recurrence of impulse displacements along a rupture / fault and groups of ruptures / faults, and also focus on physical phenomena preceding the displacements, which may suggest possible earthquake precursors in nature (e.g. (Rosenau et al., 2017, and their references). From 1960s to early 1990s, the problems of seismic event preparation and the origin of earthquake foci attracted much attention. Laboratory and field studies detected a wide range of short-term earthquake precursors, but their conceptual basis was unable to offer any solution to the problem of seismic forecasting and even raised doubts about the possibility of seismic prediction (e.g., Geller, 2007; Kogan, 1997). In that period, poor success of seismic forecasting models was due to many factors, including limited understanding of properties of the geophysical medium and insufficient knowledge of general regularities characterising the structural and dynamic development of faults. Furthermore, data collection and processing was hindered by the limited technical capacities of computers and equipment available for field and laboratory studies.

In 1990s, the knowledge advanced due to major transformations of ideas concerning the geophysical medium. The idea of a passive, deterministic, linear continuum has been replaced with the concept that described the geophysical medium as an active, discrete, non-linear system (e.g., Sadovsky et al., 1987; Pushcharovsky, 1993). Investigations have confirmed that the geophysical medium is heterogeneous; its structure is a hierarchy of blocks; and block sizes vary in a wide range, from minerals to lithospheric plates. Furthermore, self-similarity has been introduced in geophysics (e.g., Hirata, 1989; Turcotte, 1997; Seminsky, 2008).

A significant contribution to understating the development dynamics of large fault zones was brought by physical analog modeling. Based on its results, it is established that a discontinuous

internal structure of a fault zone originates from numerous ruptures and develops during their successive growth and propagation, and these ruptures join to form a major deep fault (e.g., Gzovsky, 1975; Stoyanov, 1977; Tchalenko, 1970; Wilcox et.al., 1973). In the directional evolution of faulting, several stages are distinguished by differences in strain distribution patterns and fault-forming ruptures in space and time (e.g., Sherman et al., 1991; Seminsky, 2003). More detailed investigations of the deformation dynamics of large fault zones in physical models show that these stages can be subdivided into sub-stages, and rupturing in the internal structure of a fault zone is segmental (Bornyakov and Semenova, 2011; Bornyakov et al., 2014). The deformation dynamics of individual ruptures is desplayed in the form of reactivation episodes repeating with a certain frequency. There is a regular trend in the evolution of their segmented structure from one reactivation episode to another (Bornyakov et al., 2018).

Recently, new types of displacements along faults have been instrumentally recorded, which is an important contribution to developing the deformation dynamics concept. It was previously believed that displacements along large faults took place in two deformation modes: rapid shear in fault wings (with a seismic effect), and long-term, slow, aseismic creep. Today, in addition to creep, other types of slow displacement (also termed as offset, shearing, shifting, slip) along faults are known. Such displacements differ in duration and generate seismic waves in a wide range of amplitudes and frequencies (Peng and Gomberg, 2010). Slow slip events were firstly attributed to subduction zones (Rogers and Dragert, 2003; Obara and Hirose, 2006; Brown et al., 2009); however, they can occur also in large fault zones of other types (Nadeau and Dolenc, 2005).

Although a solid classification of slow displacements and related seismic events is still lacking, the following types are generally recognized: silent earthquake, episodic tremor and slip, episodic creep event, slow slip event, low-frequency earthquake, and very low-frequency earthquake (Katsumata and Kamaya, 2003; Shelly et al., 2007; Peng and Gomberg, 2010; Sekine, 2010; Wei et al., 2013). Many studies show that slow slip events are generated / triggered by strong earthquakes; however, it is also found that slow displacements can also occur in aseismic periods (Gomberg et al., 2008; Idehara et al., 2014; Sun et al., 2015).

Attempts to solve the problem of earthquake prediction have faced new perspectives with the introduction of the synergism concept (Haken, 1977; Kondepud and Prigozhin, 1998). In its terms, a fault is a single open nonequilibrium dynamic system; an earthquake generated by a fault is a self-organized criticality (SOC) (Bak and Tang, 1989); and cooperative behavior is typical of the deformation process right before seismic reactivation of a fault (Feder, 1988; Feder and Feder, 1991; Olami et al., 1992; Ciliberto and Laroche, 1994). The SOC model is supported by simulations of seismic reactivations of faults and stick-slip mechanism (Ma et al., 2012, 2014; Zhuo et al., 2013; Guo et al., 2020).

In the above-mentioned publications, deformation is described as a process that precedes fault reactivation and develops during the metastable and meta-instable stages. After the metastable stage (time interval O–A in analysed. 1), dynamic instability takes place as a slip impulse along the fault (time interval A–B1–B2 in Fig. 1). The meta-instable stage includes two substages, early and late (MIS-I and MIS-II, respectively), which characteristic feature is the autowave nature of deformation (Ma et al., 2012, 2014; Sobolev and Ponomarev, 2003). During MIS-I (time interval A–B1 in Fig. 1), numerous strain micro-foci begin to emerge on the fault plane, i.e. some segments of the fault become active. These isolated active segments slowly grow and randomly join with each other. As a result, the fault zone is gradually differentiated into the areas with relatively high and low volume strain values. During MIS-I, tremor-like displacements occur locally along the fault segments (Guo et al., 2020). During MIS-II (time interval B1–B2 in Fig. 1), segmentation accelerates. At point B2, all the segments join with each other, and dynamic slip takes place along the fault. A complete linkage of the segments is preceded by their short-term self-organization. The onset of the linkage is accompanied by the generation and propagation of a localized deformation front (Guo et al., 2020). These effects, observed in the laboratory experiments, are indirectly confirmed in nature by the cooperative behavior of microseisms observed before strong earthquakes (Sobolev et al., 2010; Lyubushin, 2012) and anomalies of ultra-low frequency (ULF) electromagnetic emissions (Schekotov et al., 2008, 2017).

Here, we present results of analog modeling of stick-slip process along a large fault in an elastic-viscoplastic model. Our experiments show that the fault is periodically reactivated

due to the fault segmentation mechanism that is investigated in detail. The modeling data allows distinguishing stable, meta-stable, and meta-instable stages of stick-slip process.

For comparison with modeling results, we interpret rock deformation monitoring data from the South Baikal geodynamic polygon, using records taken six days before the Bystraya earthquake of September 21, 2020.

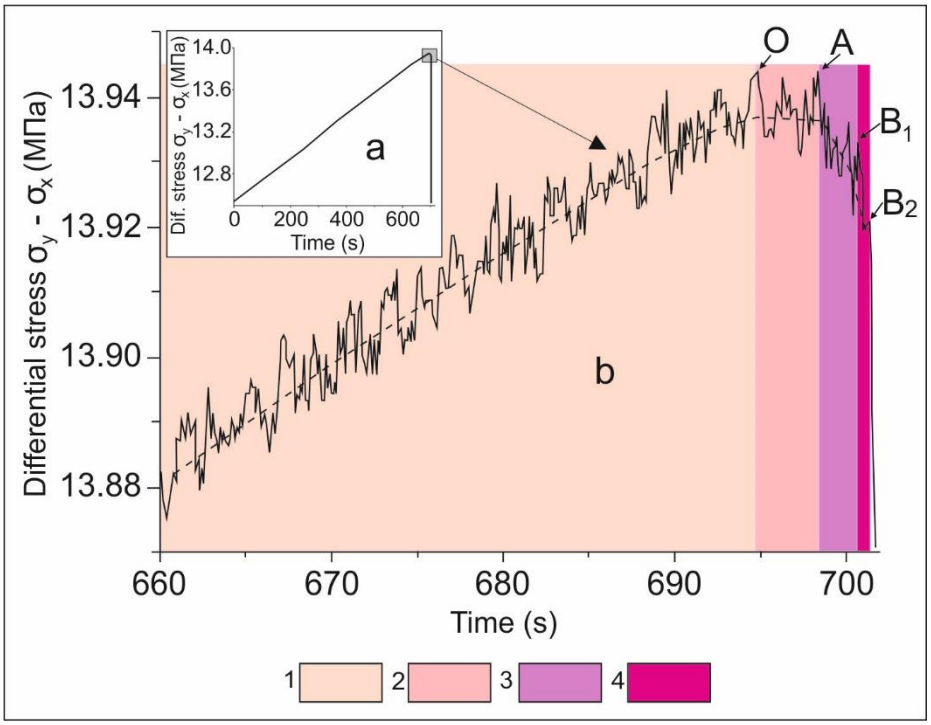

Fig. 1. Differential stress-time graph (a) and zoomed-in segment of the graph (b) showing differential stress variations during stages: up to point O – stable stage (1); from point O to A – meta-stable stage (2); from point A to B_1 – early meta-instable sub-stage (MIS-I) (3); from point B_1 to B_2 – late meta-instable sub-stage (MIS-II) (4).

Рис. 1. Дифференциальный график зависимости напряжения от времени (а) и увеличенный участок графика (b). Панель *б* показывает изменение дифференциального напряжения на стадиях: до точки О – стабильная стадия (1); из точки О до точки А – метастабильная стадия (2); от точки А до точки B_1 – ранняя метанестабильная подстадия (МИС-I) (3); от точки B_1 до B_2 – поздняя метанестабильная подстадия (МИС-II) (4).

Modeling techniques

Model scaling

Our modeling experiments aim to investigate stick-slip along a large fault and analyse its development dynamics in detail. Our procedure differs from the methodology adopted by Rosenau et al. [2009], Caniven et al. [2015] and Corbi et al. [2013] for similar experiments, who considered two different timescales for the interseismic and coseismic phases. We specify boundary conditions for only the interseismic phase.

The boundary conditions are set with respect to similarity criteria (Hubbert, 1939; Gzovsky, 1975; Sherman, 1984; Weijermars and Schmeling, 1986):

$$\eta / \rho g L T = \text{const}, \quad (1)$$

where η is viscosity, Pa s; ρ is density, kg/m³; g is free fall acceleration, m/s²; L is length, m; T is time, s.

Here, the main reological parameter is viscosity of the crust. An effective viscosity of the lower crust is at least $\sim 10^{18}$ Pa s (assuming a semi-infinite homogeneous viscous domain) (e.g., Bürgmann and Dresen, 2008; Bruhat et al., 2011). Our model simulates only the upper crust, which viscosity ranges from 10^{19} to 10^{20} Pa s.

Coefficients of similarity are as follows: $C_\eta = \eta_m/\eta_n = \sim 10^{-14}$ (viscosity); $C_\rho = \rho_m/\rho_n \sim 0.55$

(density); $C_g = g_m/g_n = 1$ (free fall acceleration); $C_l = l_m/l_n \sim 10^{-5}$ (length); $C_t = t_m/t_n \sim 2 \cdot 10^{-9}$ (time).

Considering the viscosity in the range of 10^{19} – 10^{20} Pa·s and the above-mentioned coefficients of similarity, the model material visocity is 10^5 – 10^6 Pa·s; one millimeter of the model length is similar to 100 m in nature; and one second of the experiment time is similar to 15 years in nature.

Model material

An aqueous paste of montmorillonite clay is used to simulate the elastic-viscoplastic behavior of the lithosphere subjected to long-term loading. The appropriate choice of this model material is justified by special studies reported in (Seminsky, 1986).

Experiment setup and techniques

Our physical modeling experiments are performed on the "Fault" installation (Fig. 2A). A model (1) is placed on a plexiglass sheet (2) greased with a vaseline oil (Fig. 2B). The model size: 0.65 m length x 0.45 m width x 0.1 m thickness. According to the similarity criteria, the dimensions of a simulated crustal block are as follows: 65 km length x 45 km width x 10 km thickness. Two long sides of the model are limited by fixed platens (3, 4). In the procedure to make a precut fault, we use a rectangular Plexiglas sheet (length of 0.45 m, height of 0.1 m, thickness of 0.001 m). It is manually held vertically and oriented at an angle of 40° to the direction of future movement of an active platen (6). Its vertical position kept, the sheet is manually pressed down to make a cut in the model and taken out before starting an experiment. A pre-cut fault (5) simulates a regional fault in the lithosphere (Fig. 2C). According to the criteria of similarity, its length in nature is 45 km.

In the experiment, the model is subjected to tangential compression by the platen (6) that moves at a constant speed of 10^{-5} m/s (i.e. 6.7 cm per year in nature). At the right side, another movable platen (7) is connected via springs (8) with a fixed chock platen (9). In the course of deformation of the model, this platen (7) can move towards the chock platen (9).

Before the experiment, the model surface is covered with a thin layer of fine sand. Individual sand grains act as markers for measuring displacements. Images of the model surface are taken by a Basler acA1920-40gm digital camera at a rate of one frame per second in order to record details of the process taking place within the monitored area (10).

Data processing techniques

Digital image correlation

The digital images are processed using a 2D digital image correlation method (DIC) to obtain the displacement field (Sutton et al., 2009). The DIC data processing is implemented by Strain Master software (LaVision systems) that calculates the distribution of displacement vector components and strain tensors and estimates their increments in time (Panteleev et al., 2014). Before processing, special filters are used on each image to normalize the intensity of pixels over the entire image area in order to minimize the effect of uneven illumination of photographed objects. Furthermore, all the images are calibrated by a frame with a measuring ruler, which makes it possible to refer to the real spatial scale of photographed objects and reconstruct the displacement field in millimeters (instead of pixels).

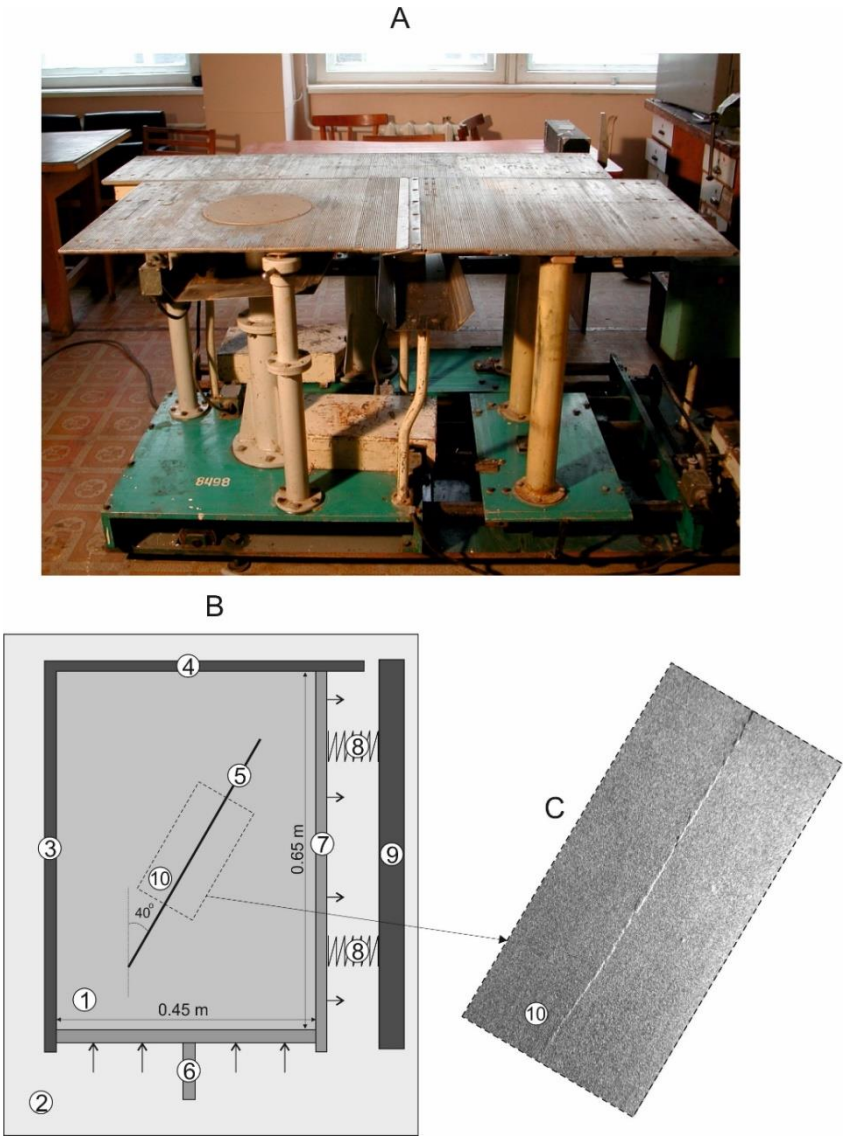

Fig. 2. Experimental installation “Fault” (*a*), schematics of experiment setup (*b*), and photo of the fault after its reactivation (*c*). Numbers – see in the text.

Рис. 2. Экспериментальная установка «Разлом» (*a*), схема экспериментальной установки (*b*) и фото разлома после его реактивации (*c*). Цифры – см. текст.

Image processing can be carried out in either integral or differential scenarios. In the integral scenario, the model deformation field is assessed by comparing every image with the first one, i.e. taken before the experiment start (Fig. 3a), and the pattern of consecutive accumulation of deformation during loading can be reconstructed. In the differential scenario, the deformation field is assessed by comparing two images taken consecutively, one after another, and an increment of deformation from one image to another is calculated.

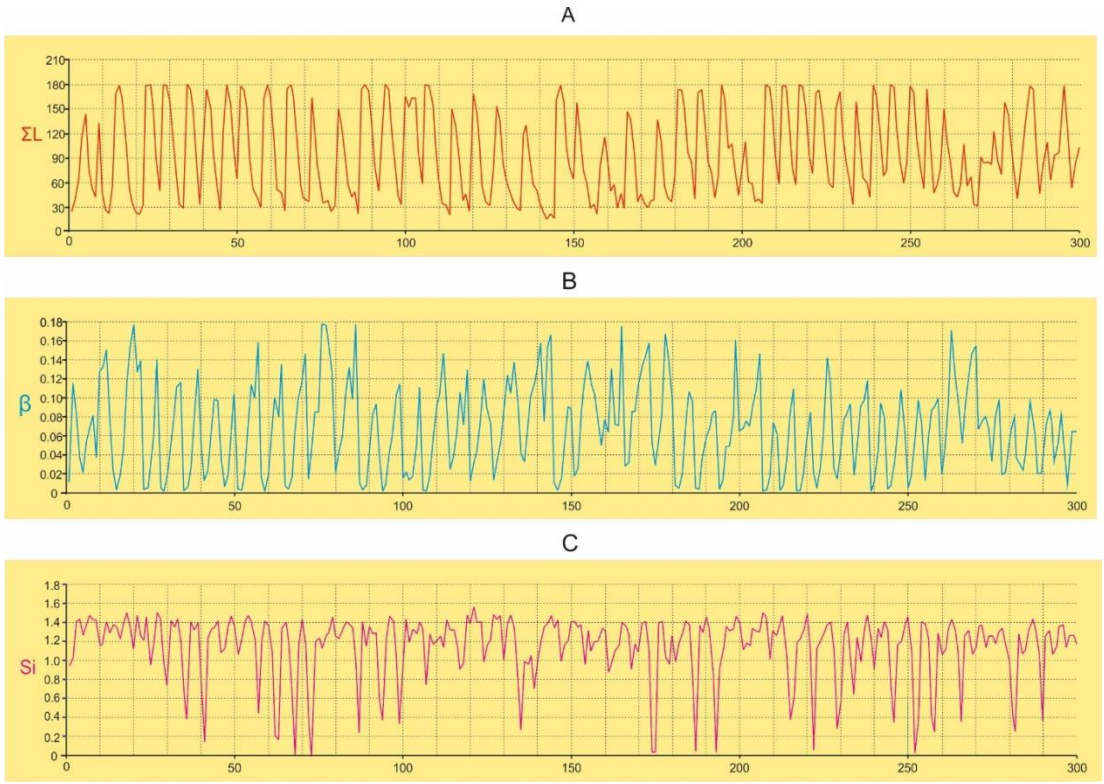

Fig. 3. Temporal changes in total length ΣL (*a*)**,** inclination angle of recurrence graph β (*b*), and information entropy Si (*c*) of active segments.

Рис. 3. Временные изменения общей длины ΣL (*a*), угла наклона рекуррентного графика β (*b*) и информационной энтропии Si (*c*) активных сегментов.

We use the differential approach for processing the images in order to clearly identify the nonlinear, non-monotonic features of deformation. Displacement and deformation fields are reconstructed under the following DIC algorithm: correlation analysis – multi-pass with a sub-window size varying from 12.8x12.8 mm to 1.6x1.6 mm; step size – 50 % of the sub-window size; correlation function – normalized, second order. At each time step, the resultant field of velocity is smoothed by a two-dimensional Gaussian filter (0.6 x 0.6 mm). A 5-minute interval of the experiment time is chosen for processing purposes. In total, 300 images were processed.

Algorithms for statistical processing of quantitative parameters

The model data processing results show that deformation takes place as left-lateral shear along the entire fault or along its individual active segments. In the fault wings, deformation occurs as localized plastic shearing along two conjugated systems of microruptures.

The calculated distribution patterns of shear deformation provide the basis to construct structural diagrams of the active segments and plastic microruptures in the fault wings. The diagrams are used to calculate their numbers (N) and lengths (Li). Initial parameters are then used to estimate their total (ΣLi) and average (L average = ΣLi/N) lengths, β value and information entropy (Si) from parameter Li.

The β value is calculated by the maximum likelihood method (Aki, 1965):

$$\beta = \lg e / L_{average} - L_{min}, \quad (2)$$

where *e* is natural logarithm base; L average is average length; L min is minimum length of active segments in the data set that yields from the analysed structural diagram. The method described in (Aki, 1965) is adapted for analysing earthquake magnitudes. Here, in equation (2), the lengths of active segments are used instead of earthquake magnitudes – this is allowable as we take into account the known rela-

tionship between fault length and earthquake magnitude (Tocher, 1956; Golitsyn, 1996).

Information entropy is calculated as follows (Brillouin, 1964):

$$Si = - \Sigma pi \cdot lg\, pi, \quad (3)$$

where p is probability.

Results

Long-term deformation dynamics

Computer processing of the images showing the model surface during deformation confirms that even under constant loading, the structural evolution of active segments and displacements along the fault takes place according to the stick-slip mechanism as described in (Brace and Byerlee, 1966). During the monitored 300-second interval, 47 displacements (i.e. activation impulses) of various intensity occurred with a time discreteness of five to ten seconds either, and either the entire fault or its major part were activated. Between the activation impulses, activity concentrated in individual segments of the fault.

Based on the 300 processed images, 300 shear strain plots were constructed. For each plot, structural diagrams of active segments were drawn up, and lengths Li were measured. These data were used to estimate the total length of active segments (ΣL), inclination angle of recurrence graph (β value), and information entropy (Si) (Fig. 3).

Short-term deformation dynamics between two activations of the entire model fault

We analysed in detail the structural evolution of the model fault and changes in parameters of its active segments between two activations of the entire fault (Fig. 4). This cycle lasts for 2 seconds in the model and simulates a seismic cycle in nature (i.e. activations correspond to seimic events). In the shear strain distribution diagram, full activation is a moment when the entire fault length within the monitored area is active. After the first activation (Fig. 4A, A′), displacements occur fragmentarily at several relatively large segments of the fault (Fig. 4B, B′).

In the next six intervals of time, segmentation develops, and the large segments are split into a series of smaller ones (Fig. 4B′– G′). The number of segments increases, their average and total lengths decrease, and the inclination angle of the recurrence graph increases (Table 1; Fig. 4C′–G′) Before the next full activation, segmentation stabilizes (Table 1; Fig. 4H, H′) and then develops in the opposite direction: the number of segments decreases, their average and total lengths increase, and the inclination angle of the recurrence graph decreases (Table 1; Fig. 4I, I′).

Short-term deformation dynamics in the model fault wing

Active plastic microruptures in the model fault wing were analysed separately to reveal their short-term deformation dynamics. Figure 5 shows a fragment of the shear strain distribution diagram at the moment when the entire fault is activated (see Fig. 4J, J′). Numerous conjugated plastic microruptures of two strikes are present in the fault wing. Linearly localized shear strain maxima were detected. By analogy with the active segments, the number and lengths of plastic microruptures were determined, then the total and average lengths and information entropy were estimated (Table 1). In the discussion below, we compare graphs showing changes in parameters of active segments and plastic microshears with time.

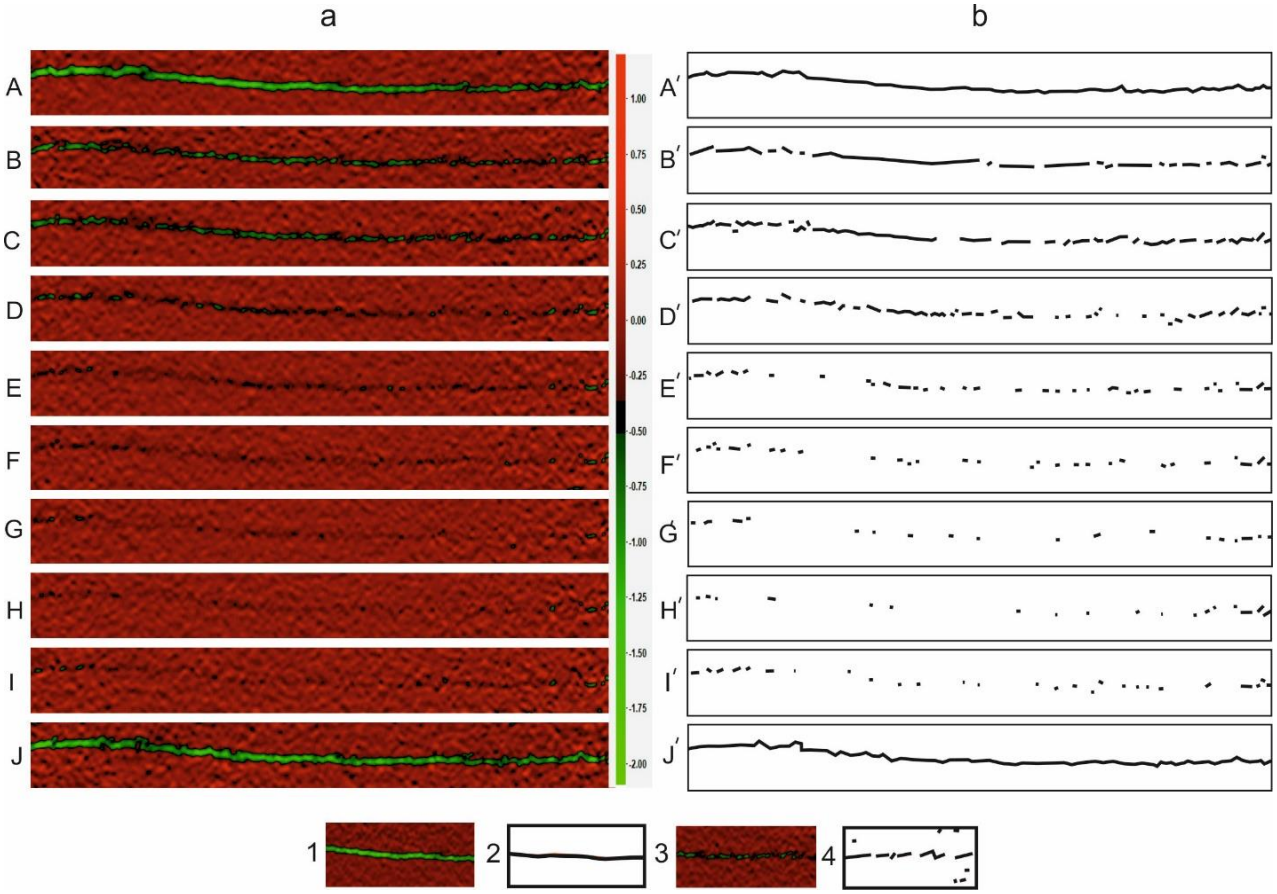

Fig. 4. Shear strain distribution diagram illustrating the structural evolution between two reactivations of the model fault (*a*) structural scheme of activated fault and its active segments (*b*). 1 – active fault according to DIC data processing data (A and J); 2 – active fault in structural schemes (A′ and J′); 3 – active fault segments according to DIC data processing data (B–I); 4 – active fault segments in schemes B′–I′.

Рис. 4. Диаграмма распределения деформации сдвига, иллюстрирующая структурную эволюцию между двумя активациями модельного разлома (*a*) и структурная схема активированного разлома и его активных участков (*b*). 1 – активный разлом по данным обработки данных DIC (A и J); 2 – активный разлом в структурных схемах (A′ и J′); 3 – участки активных разломов по данным обработки данных DIC (B–I); 4 – участки активных разломов на схемах Б′–I′.

Short-term deformation dynamics in the model fault wing

Active plastic microruptures in the model fault wing were analysed separately to reveal their short-term deformation dynamics. Figure 5 shows a fragment of the shear strain distribution diagram at the moment when the entire fault is activated (see Fig. 4J, J′). Numerous conjugated plastic microruptures of two strikes are present in the fault wing. Linearly localized shear strain maxima were detected. By analogy with the active segments, the number and lengths of plastic microruptures were determined, then the total and average lengths and information entropy were estimated (Table 1). In the discussion below, we compare graphs showing changes in parameters of active segments and plastic microshears with time.

Table 1

Parameters of the model fault segments and plastic microruptures, and their changes between two full reactivations

Time, s	Number of segments	Total length of segments, mm	Average length of segments, mm	Information entropy of the segments lengths
Parameters of active segments				
0 (FA)*	1	180	180	-
1	24	164	3.1	0.11
2	36	109	1.1	0.16
3	36	128	1.2	0.38
4	34	78	0.7	0.52
5	28	48	0.35	1.39
6	18	30	0.3	1.11
7	18	29	0.35	1.54
8	27	49	0.4	0.87
9 (FA)*	1	180	180	-
Parameters of active plastic microruptures in the fault wing				
0 (FA)*	210	1100	10.48	2.245
1	162	745	9.2	2.180
2	202	995	9.85	2.240
3	255	1307	10.26	2.325
4	260	1300	10.0	2.234
5	272	1347	9.91	2.237
6	235	1140	9.7	2.229
7	231	1200	10.39	2.227
8	279	1450	10.39	2.238
9 (FA)*	268	1173	8.75	2.236
0 (FA)*	210	1100	10.48	-

*Note: FA – full activation.

Discussion and findings based on the modeling results

It is known from laboratory experiments with geologic materials (Brace and Byerlee, 1966), and our experiments confirm that in elastic-viscoplastic models, displacements along the existing fault develop non-uniformly even under constant loading and evolve according to the stick-slip mechanism. At the moments of activation impulses, displacements occur along the entire fault or along its major part. Between the activation impulses, activity concentrates in individual segments of the fault (Fig. 4).

Considering the stick-slip process developing in the model in terms of repeated self-organized criticality (Bak and Tang, 1989), one should expect that immediately before the complete activation of the fault, as soon as the critical stress level on the fault plane is reached, the system of active segments transforms to the state of self-organization (Ma et al., 2012, 2014). The self-organization process is preceded by the transition stage when the system reaches its current equilibrium or a metastable state with an increase in the degree of disorder (Kondepudi and Prigogine, 1998). An indicator of the degree of disorder in open systems is thermodynamic entropy or its statistical analogue, information entropy Si (Brillouin, 1964; Zubarev et al., 2002; Gudmundsson and Mohajeri, 2013). Our experiments show that changes in Si with time are consistent with the above conclusions (Fig. 3). The moments, when the entire fault is activated, correspond to the maximum values of ΣL and correlate with the maximum values of information entropy (76 %).

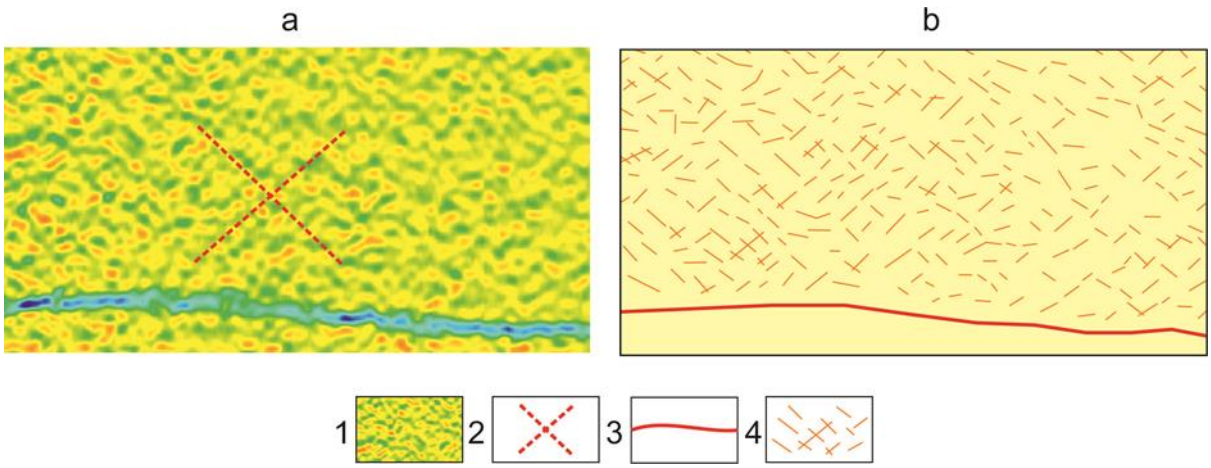

Fig. 5. Plastic microruptures in the model fault wing (blue line – fault) (a) and structural diagram (b). Legend: 1 – shear strain maximums corresponding to plastic microruptures; 2 – two main strikes of microruptures; 3 – model fault; 4 – plastic microruptures in the structural scheme.

Рис. 5. Пластические микроразрывы в модельном крыле разлома (синяя линия – разлом) (a) и структурная схема (b). Условные обозначения: 1 – максимумы сдвиговых деформаций, соответствующие пластическим микроразрывам; 2 – два основных простирания микроразрывов; 3 – модельный разлом; 4 – пластические микроразрывы в конструктивной схеме.

The evolution of active segments and plastic microshears can be traced in detail from one activation of the fault to another by changes in their parameters, as shown in Table 1 and Figure 5. With respect to these changes, we distinguish two trends of the model fault segmentation: regressive (0s–7s), and progressive (7s–9s) (see Table 1). The progressive segmentation period is significantly shorter than the regressive one. Furthermore, the shorter is progressive segmentation, the more intense is fault activation, and almost the entire fault is activated. Vice versa, with an increase in the duration of the progressive segmentation, activation of the fault is less intense, and some segments of the fault are most likely to remain inactive.

We constructed graphs showing changes in parameters of active segments and plastic microshears (N, ΣL, L average and Si) with time (Fig. 6). By comparing these graphs, we reveal that the deformation dynamics is different at the fault itself and in its wings. This difference is clearly reflected in the behavior of parameters ΣL and L average. After the first full activation, the number, total and average lengths of plastic microshears decrease for a short time, while the values of Si increase. Later on, up to the next full activation, the values of N, ΣL, L average and Si generally increase, with slight variations. Considering the segments and plastic microshears, changes in their parameters ΣL and L average are almost anti-phased in time.

The regressive segmentation leads to gradual fragmentation of large segments into smaller ones and their degeneration as some of them become passive. This trend is reflected in a decrease in the number of large segments and a decrease in their total and average lengths (Fig. 6a, b, c). Information entropy increases during the regressive segmentation, which means an increasing degree of chaos in the distribution of fault segments by their lengths (Fig. 6d). By the end of the regressive segmentation period, stresses reach their maximum values, but the fault is still meta-stable, which means that only its individual short segments are active. Such segments are evenly distributed along the fault strike.

The fault becomes newly activated when the progressive segmentation begins in the early meta-instable sub-stage (MIS-I). Its activity is manifested by an increase in the number of active segments and plastic microshears to a certain critical density, while their spatial patterns become more chaotic. In MIS-II, the number of segments decreases as they rapidly grow and join with each other to form larger segments, up to full activation of the entire fault.

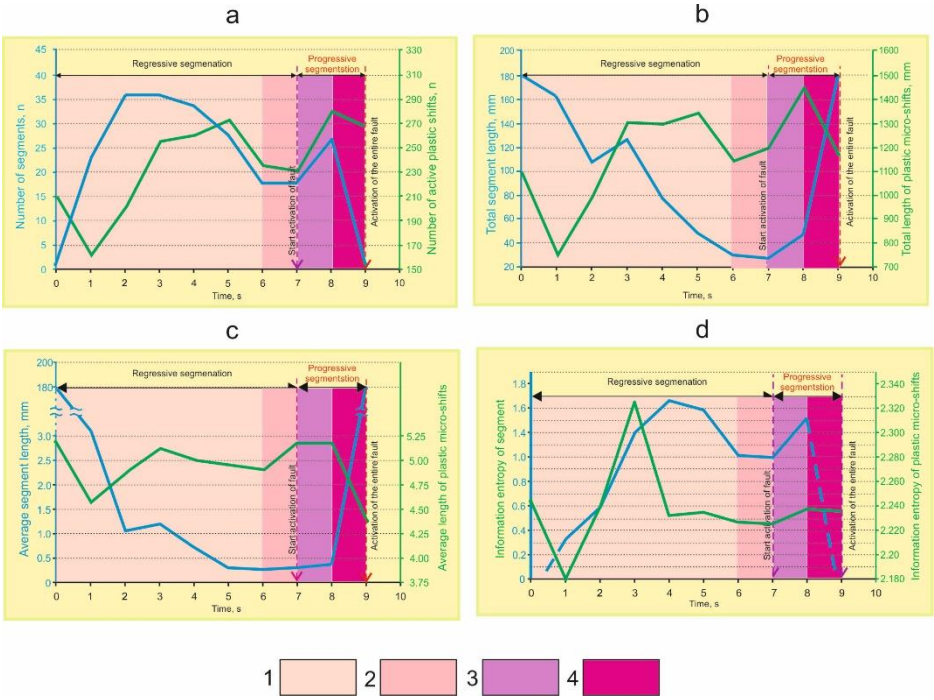

Fig. 6. Changes in parameters N, ΣL, L average and Si with time. (a) Number of segments, N; (b) total length, ΣL; (c) and average length, $L_{average}$; (d) informational entropy, Si. Stages of the stick-slip preparation at the model fault: 1 – stable; 2 – meta-stable; 3, 4 – early (3) and late (4) meta-instable (MIS-I and MIS-II, respectively).

Рис. 6. Изменение параметров N, ΣL, L в среднем и Si во времени. Количество сегментов N (a), общая длина ΣL (b), средняя длина, $L_{средняя}$ (*c*) и информационная энтропия Si (d). Стадии прерывистой подготовки на модельном разломе: 1 – стабильная; 2 – метастабильный; 3, 4 – ранняя (3) и поздняя (4) метанестабильность (МИС-I и МИС-II соответственно).

The above-described dynamics of the structural evolution of active fault segments in the elastic-viscousplastic model during the meta-instable stage, including MIS-I and MIS-II, agrees well with the dynamics described by Ma et al. (2012, 2014) and Guo et al. (2020) who performed stick-slip modeling experiments using granodiorite specimens.

After stresses decrease in the fault wing, active plastic microshears reduce in number, and their total and average lengths are also reduced, while their spatial patterns become less chaotic, as reflected in a decrease in Si values (Fig. 6d).

Our key findings are summarized as follows:

– Activation of a fault is preceded by its transition to the meta-stable state;

– The fault is periodically activated due to the segmentation mechanism;

– Progressive segmentation of the fault takes place during the early and late meta-instable sub-stages (MIS-I and MIS-II);

– The short-term deformation dynamics differs in the model fault wing and at the entire fault;

– During the MIS, the deformation process accelerates, and a localized deformation front occurs in the fault wing before the occurrence of dynamic stick-slip along the fault, and this front propagates towards a location of future seimogenic displacements.

These findings should be taken into account when processing and analysing strain monitoring data from a fault zone with potential seismic hazard – data analyses should be conducted separately for the fault itself and its wings.

Our modeling results can be useful for developing seismic forecasting techniques and improving earthquake prediction. For instance, when monitoring a seismically active fault, it is possible to detect its meta-stable state from autowave phenomena in time series of various geophysical parameters, which are indirectly re-

flected in high values of information entropy. In the areas of potential earthquake foci, the progressive segmentation during the meta-instable stage can be diagnosed instrumentally by broadband seismic stations launched within or near a source area. In an earthquake-prone area, a network of deformation monitoring stations can detect the formation of a localized deformation front and contribute to providing a better prediction of earthquake foci locations.

Natural seismic event as a case for verification of the model results

To verify the stages of preparation of dynamic stick-slip along the model fault, we analysed deformation monitoring data related to preparation of the Bystrinsky earthquake (*Mw* 5.4) occurred September 21, 2020 at18:04 UTC or September 22, 2020 at 02:04 AM Irkutsk time) in the southern Baikal region, Russia (51° 77/, 103° 43 according to the data from the Talaya Seismic Station owned by the Baikal Branch of UGS RAS). Its epicenter was located at a distance of 18 km from the station. This seismic event is reported in detail in (Bornyakov et al., 2021) (Fig. 7).

Preparation of the Bystrinsky earthquake is reflected in rock deformation monitoring data from the Talaya deformation monitoring site (part of the Talaya Station area, Fig. 8). The strain records were taken by a permanently installed monitoring unit of the author's design; its technical characteristics are described in (Salko and Bornyakov, 2014).

Six days before the earthquake, eight sensors out of ten registered changes in the rate of rock deformation accumulation. The most distinct anomalous changes in the deformation process were recorded by rod sensors 1, 4 and 8 – they were oriented towards the future focal area of the earthquake. Figure 9 (a) illustrates a time series of strain records taken by sensor 8 from September 05, 2020 to October 02, 2020. The rock deformation decreased from September 5 to September 16, and then began to increase. Closer to the day of the earthquake occurrence, the deformation accelerated, as evidenced by the graph showing daily strain increments (Fig. 9b). After the earthquake, the rock deformation began to decrease again, and gradually reduced to the background values (Fig. 9).

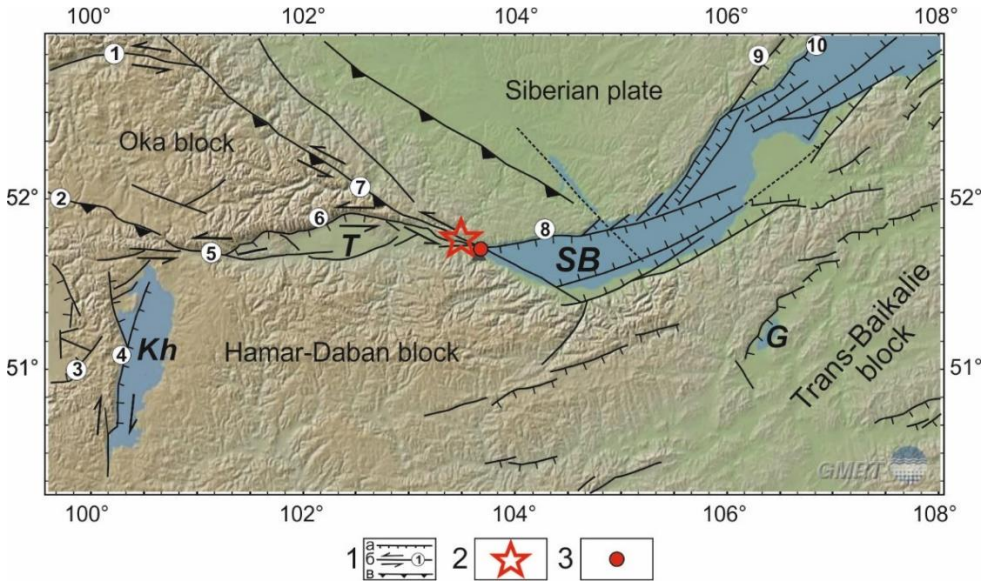

Fig. 7. Neotectonic structures in the southern Baikal region. Legend: 1 – active faults: *а* – normal, *б* – strike-slip, *в* – reverse; 2 – epicenter of the Bystraya earthquake; 3 – Talaya deformation monitoring site. Rift basins (letters): SB – South Baikal. Kh – Khubsugul, G – Gusinoozersk. Main active faults (numbers in circles): 1 – Zhombolok, 2 – South Oka, 3 – Darkhat, 4 – Khubsugul, 5 – Baikal-Mondy, 6 – Tunka, 7 – Main Sayan, 8 – Obruchev, 9 – Primorsky, 10 – Morskoy.

Рис. 7. Неотектонические структуры Южного Прибайкалья. Условные обозначения: 1 – активные разломы: *а* – сброс, *б* – сдвиг, *в* – взброс; 2 – эпицентр Быстринского землетрясения; 3 – площадка мониторинга деформаций Талая. Рифтовые бассейны (буквы): SB – Южный Байкал. Kh – Хубсугул, G – Гусиноозерск. Основные действующие разломы (цифры в кружках): 1 – Жомболокский, 2 – Юж-

но-Окинский, 3 – Дархатский, 4 – Хубсугульский, 5 – Байкало-Мондинский, 6 – Тункинский, 7 – Главный Саянский, 8 – Обручевский, 9 – Приморский, 10 – Морской.

The deformation behavior during the preparation of the Bystrinsky earthquake is a good example in support of the meta-stable and meta-instable stages of stick-slip preparation in the modeling experiments described in (Ma et al., 2012, 2014) and this paper. The MIS began at the moment when the maximum load value was reached (at point O on the load-time curve in Fig. 1). Transition to meta-instability started when isolated segments of the local fault became active. The MIS included MIS-I and MIS-2 (A–B1, and B1– B2, respectively, in Fig. 1). In MIS-I (September 16 to 20), stresses slowly and gradually decreased due to a gradual increase in the number of fault segments, i.e. slowly accelerated deformation took place. During MIS-I, tremor-like slip occurred (Fig. 9c). In MIS-II (September 20), synergism is observed – the deformation process was considerably accelerated, and then a dynamic slip impulse took place along the fault. According to (Ma et al., 2012, 2014), synergistic effects occur when the quasi-static state is transformed into a quasi-dynamic one via cooperative interaction of the active segments, their rapid growth in length and linkage with each other. In MIS-II, short-term deceleration occurred right before the main seismic shock of September 22, 2020. Thus, the deformation dynamics recorded at the Talaya site six days before the earthquake is fully consistent with our concept of the early and late meta-instability sub-stages.

Considering the same earthquake, an additional argument in favour of this concept can be found in specific variations of the information entropy calculated from the time series of strain records in a 1-day window with a 1-day shift (Fig. 9d). In the graph, a sharp decrease in the information entropy begins on September 13, i.e. two to three days before deformation starts increasing. This means that during these two or three days, there was a change in the dynamic state of the fault-block medium in the source area, as well as a transition from meta-stability to meta-instability of the deformation process.

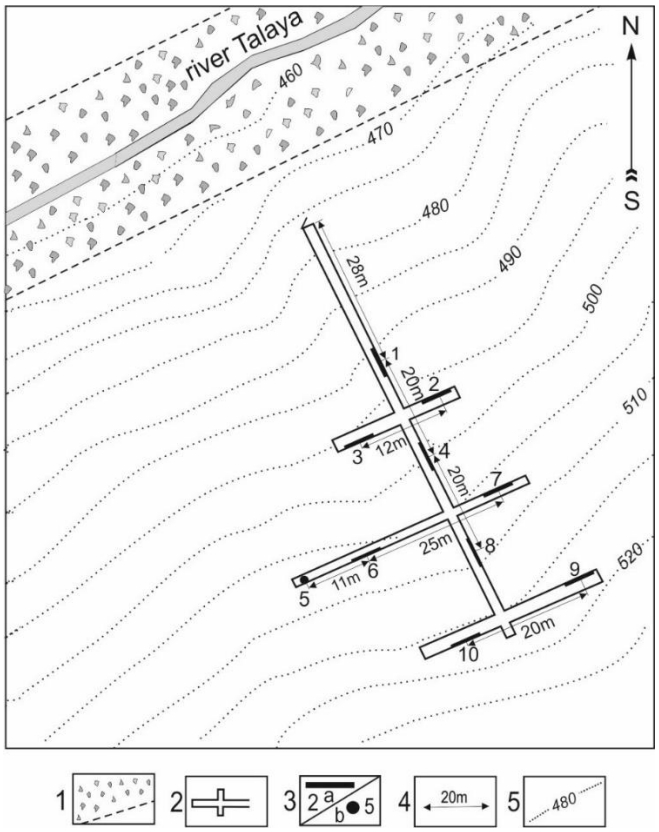

Fig. 8. Sketch of the Talaya deformation monitoring site. 1 – fault zone; 2 – contours of a mine shaft; 3 – rod sensors installed in horizontal (a) and vertical (b) positions in the mine shaft, and their numbers (1–10); 4 – distance between rod sensors; 5 – topography line and elevation.

Рис. 8. Схема участка деформационного мониторинга Талая. 1 – зона разлома; 2 – контуры шахтного ствола; 3 – стержневые датчики, установленные в горизонтальном (a) и вертикальном (b) положениях в стволе шахты, и их номера (1–10); 4 – расстояние между стержневыми датчиками; 5 – линия рельефа и высота.

Thus, the deformation monitoring data allow us to clearly determine the final stage, during which the Bystrinsky earthquake was prepared. This stage agrees well with the meta-instable stage (including MIS-I and MIS-II) in our stick-slip modeling experiments. Having compared the model and natural data, we suggest that meta-instability of a fault, manifested by specific anomalous deformation dynamics at the fault itself and in its wings, can be considered as a short-term precursor of earthquakes.

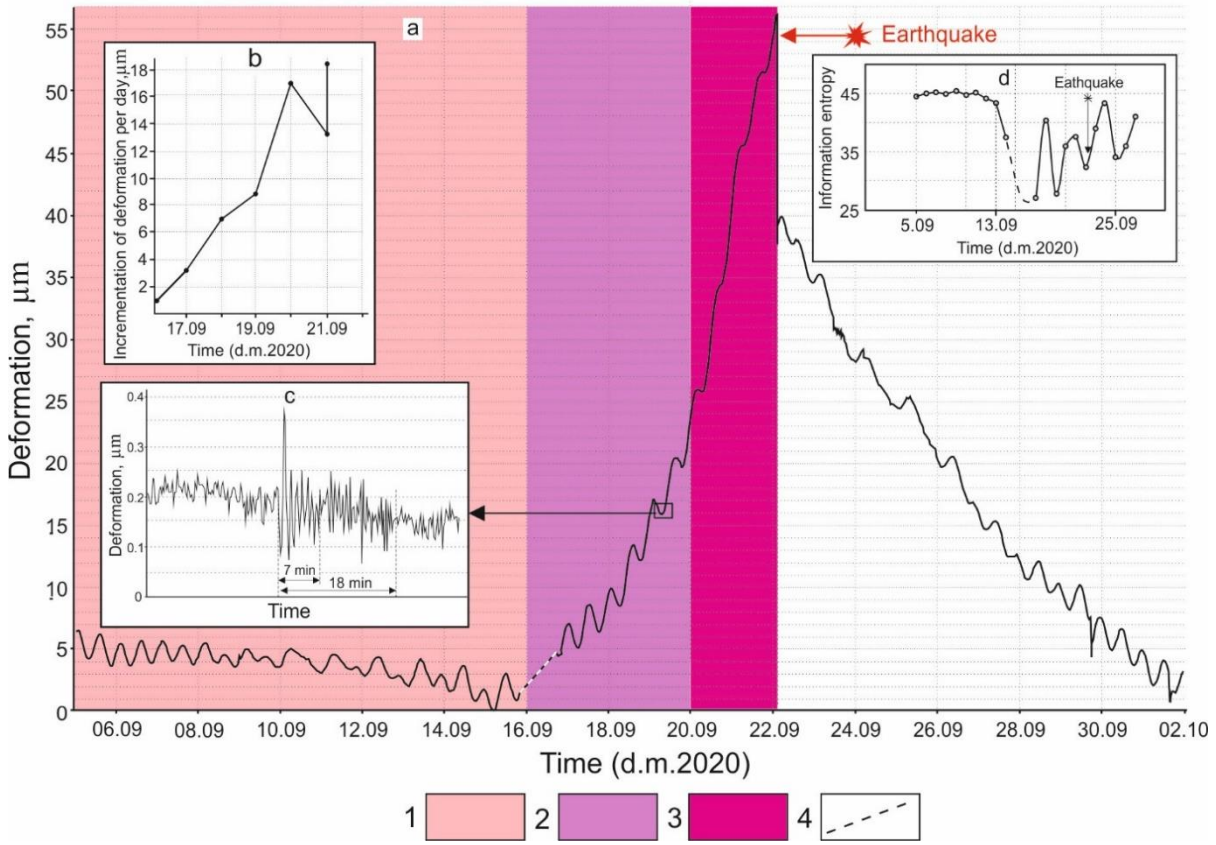

Fig. 9. Rock deformation at the Talaya monitoring site before the Bystraya earthquake (a), graph of daily strain increment (b), reflection of tremor-like slip in the strain data (c), and information entropy graph (d). Stages of earthquake preparation: 1 – meta-stable; 2, 3 – early (3) and late (4) meta-instable (MIS-I and MIS-II, respectively); 4 – no data.

Рис. 9. Деформация горных пород на полигоне Талая перед Быстринским землетрясением (a), график суточного прироста деформации (b), отражение трemороподобной подвижки в данных деформации (c) и график информационной энтропии (d). Стадии подготовки землетрясений: 1 – метастабильная; 2, 3 – ранняя (3) и поздняя (4) метанестабильная (МИС-I и МИС-II соответственно); 4 – нет данных.

Conclusions

In the experiments aimed at physical modeling of stick-slip along the precut large fault, we have discovered a mechanism responsible for the preparation and occurrence of periodic full activations of the fault. According to the modeling results, the major mechanism is segmentation that differentiates the fault along its strike into a series of alternating active and passive segments. The segmentation pattern is regular in time, and two trends are distinguished – regressive and progressive segmentation of active segments. In the period of regressive segmentation, stick-slip occurs locally along several relatively large segments of the fault, which subse-

quently break up into a series of smaller ones, and most of them gradually become passive. The progressive segmentation develops in the opposite direction: the existing and newly formed small segments join with each other to form larger ones, and finally the entire fault becomes active. Our experiment results clearly show that the progressive segmentation of the fault in the elastic-viscoplastic model agrees well with the segmentation during the meta-instability stage identified from the stick-slip models using granodiorite specimens (Ma et al., 2012, 2014; Guo et al., 2020).

Variations in activity of the fault segments are closely related to stress variations in the area around the fault, wherein the plastic microshears are observed. Our experiments show that the deformation dynamics is considerably different in the active segments and the plastic microshears in the fault wings. Furthermore, there are significant differences in the deformation dynamics within different time intervals. Therefore, it should be emphasised that proper statistical estimates for seismic forecasting can yield only from a methodologically correct approach – it is critical to ensure that considering a fault zone of potential seismic hazard, strain and seismic data are analysed separately for the fault itself and its wings.

We have compared the laboratory modeling results and our interpretation of the rock deformation monitoring data from the South Baikal geodynamic test site. Based on the analysis of the strain records taken six days before the Bystrinsky earthquake of September 22, 2020, we conclude that specific features of the anomalous rock deformation recorded in nature are fully similar to the features of deformation along the model fault during the meta-instable stage. There are thus grounds to suggest that the meta-instable stage can be considered as a short-term precursor of an earthquake. An important consequence of our stick-slip modeling experiments is a confirmed possibility of using strain monitoring records from fault zones and detailed analyses of their deformation dynamics for predicting the occurrence of seismic events.

Acknowledgments

The study was carried out under the project "Modern geodynamics, mechanisms of destruction of the lithosphere and dangerous geological processes in Central Asia", No FWEF-2021-0009. This work involved the South Baikal instrumental complex for monitoring hazardous geodynamic processes in frame of the Centre of Geodynamics and Geochronology at the Institute of the Earth's Crust, Siberian Branch of the Russian Academy of Sciences.

References

Aki K. Maximum likelihood estimate of bin the formula logN = a−bm and its confidence limits // Bulletin of the Earthquake Research Institute, University of Tokyo. 1965. Vol. 43. P. 237–238.

Bak P., Tang C. Earthquakes as a self-organized critical phenomenon // Journal of Geophisical Research. 1989. Vol. 94, No. B11. P. 15635–15637. doi.org/10.1029/JB094iB11p15635

Bornyakov, S. A., Dobrynina, A. A., Seminsky, K. Zh., Sankov, V. A., Radziminovich, N. A., Salko, D. V., Shagun, A. N. Bystrinsky earthquake in the Southern Pribaikalye (21.09.2020, MW =5.4): general characteristic, basic parameters and deformation signs of the transition of the fosi to the meta-unstable state // Doklady Earth Sciences. 2021. Vol. 498, No. 1. P. 84–88. doi.org/10.31857/S2686739721050042

Bornyakov S.A., Semenova N.V. Dissipative processes in fault zones (based on physical modeling results) // Russian Geology and Geophysics. 2011. Vol. 52, No. 6. P. 676–683. doi.org/10.1016/j.rgg.2011.05.010

Bornyakov S.A., Seminsky K.Z., Buddo V.Y., Miroshnichenko A.I., Cheremnykh A.V., Cheremnykh A.S., Tarasova A.A. Main regularities of faulting in lithosphere and their application (based on physical modeling results) // Geodynamics and Tectonophysics. 2014. Vol. 5, No. 4. P. 823–861 (in Russian). doi.org/10.5800/GT-2014-5-4-0159.

Bornyakov S.A., Panteleev I.A. The segmentation mechanism of periodic reactivation of a fault: results of physical modeling // Doklady Earth Sciences. 2018. Vol. 482, No. 1. P. 1178–1181. doi.org/10.1134/S1028334X18090039

Brace W.F., Byerlee J.D. Stick-slip as a mechanism for earthquake // Science. 1966. Vol. 153. P. 990–992.

Brillouin L. Science and Information Theory. Acad. Press Publ., New York, 1964. 164 pp.

Brown J.R., Beroza G.C., Ide S., Ohta K., Shelly D.R., Schwartz S.Y., Rabbel W., Thorwart M., Kao H. Deep low-frequency earthquakes in tremor local-

ize to the plate interface in multiple subduction zones // Geophysical Research Letters. 2009. Vol. 36, No. L19306. doi:10.1029/2009GL040027

Bruhat L., Barbot S., Avouac J.-P. Evidence for postseismic deformation of the lower crust following the 2004 Mw6.0 Parkfield earthquake // J. Geophys. Res. 2011. Vol. 116, No. B08401. doi:10.1029/2010JB008073.

Bürgmann R., Dresen G. Rheology of the lower crust and upper mantle: Evidence from rock mechanics, geodesy, and field observations // Annu. Rev. Earth Planet. Sci. 2008. Vol. 36. P. 531–567. doi:10.1146/annurev.earth.36.031207.124326.

Caniven Y., Dominguez S., Soliva R., Cattin R., Peyret M., Marchandon M., Romano C., Strak V. A new multilayered visco-elasto-plastic experimental model to study strike-slip fault seismic cycle // Tectonics. 2015. Vol. 34, No. 2. P. 232–264. doi:10.1002/2014TC003701.

Ciliberto S., Laroche C. Experimental evidence of self-organization in the stick-slip dynamics of two rough elastic surface // Journal de Physique. , 1994. Vol. 4, P. 223–236. doi:10.1051/jp1:1994134

Corbi F., Funiciello F., Moroni M., van Dinther Y., Mai P.M., Dalguer L.A., Faccenna C. The seismic cycle at subduction thrusts: 1.Insights from laboratory models // J. Geophys. Res. Solid Earth. 2013. Vol. 118. P. 1483–1501. doi:10.1029/2012JB009481.

Feder J. Fractals. Plenum Press, New York, 1988. doi.org/10.1007/978-1-4899-2124-6.

Feder J.S., Feder J. Self-organized criticality in stick-slip process // Physical Review Letters. 1991. Vol. 66, No. 20. P. 2669–2672. doi.org/10.1103/PhysRevLett.66.2669.

Haken H. Synergetics. An Introduction. Springer-Verlag, Berlin–Heidelberg–New York, 1977. 325 pp.

Hirata T. Fractal dimension of fault systems in Japan: Fractal structure in rock fracture geometry at various scales // Pure Applied Geophysics. 1989. Vol. 131. P. 157–170. doi:10.1007/BF00874485.

Hubbert M.K. Theory of scale models as applied to the study of geologic structures // Geological Society of America Bulletin. 1937. Vol. 48. P. 1459–152.

Geller R.J. Earthquake prediction: a critical review // Geophysical Journal International. 2007. Vol. 131, No. 3. P. 425–450. doi.org/10.1111/j.1365-246X.1997.tb06588.x

Golitsyn G.S. Earthquakes from the standpoint of similarity theory // Doklady Earth Sciences. 1996. Vol. 346, No. 4. P. 563–539.

Gomberg J., Rubinstein J.L., Peng, Z.G., Creager K.C., Vidale J.E., Bodin P. Widespread triggering of nonvolcanic tremor in California // Science. 2008. Vol. 319, No. 5860. P. 173. doi.org/10.1126/science.1149164.

Gudmundsson A., Mohajeri N. Relations between the scaling exponents, entropies, and energies of fracture networks // Bulletin de la Societe Geologique de France. 2013. Vol. 184, No. 4–5. P. 373–382. doi.org/10.2113/gssgfbull.184.4-5.373.

Guo Y., Zhuo Y., Liu P., Chen S., Ma J. Experimental study of observable deformation process in fault meta-instability state before earthquake generation // Geodynamics and Tectonophysics. 2020. Vol. 11, No. 2. P. 417–430. doi.org/10.5800/GT-2020-11-2-0483.

Gzovsky M.V. Fundamentals of tectonophysics. Nauka, Moscow, 1975. 536 pp. [Гзовский М.В. Основы тектонофизики. М.: Наука, 1975. 536 с.]

Idehara K., Yabe S., Ide S. Regional and global variations in the temporal clustering of tectonic tremor activity // Earth Planets Space. 2014. Vol. 66, No. 66. doi.org/10.1186/1880-5981-66-66.

KaganY.Y. Are earthquakes predictable? // Geophysical Journal International. 1997. Vol. 131. P. 505–525. doi.org/10.1111/j.1365-246X.1997.tb06595.x.

Katsumata A., Kamaya N. Low-frequency continuous tremor around the Moho discontinuity away from volcanoes in the southwest Japan // Geophysical Research Letters. 2003. Vol. 30, No. 1. P. 1020. doi:10.1029/2002GL0159812.

Kondepudi, D., Prigogine, I., 1998. Modern Thermodynamics: From Heat Engines to Dissipative Structures: Second Edition. John Wiley and Sons, Oxford, 506 pp.

Ma J., Guo Y, Sherman S. I. Accelerated synergism along a fault: A possible indicator for an impending major earthquake // Geodynamics and Tectonophysics. 2014. Vol. 5, No. 2. P. 387–399. doi.org/10.5800/GT-2014-5-2-0134.

Ma J., Sherman S.I., Guo Y.S. Identification of meta-instable stress state based on experimental study of evolution of the temperature field during stick-slip instability on a bending fault // Science China Earth Sciences. 2012. Vol. 55. P. 869–881. doi.org/10.1007/s11430-012-4423-2.

Myachkin V.I., Kostrov B.V., Sobolev G.A., Shamina O.G. Fundamentals of the physics of earthquake foci and fore-runners. In M.A. Sadovsky (Ed.), Physics of Earthquake Focus. Nauka, Moscow, 1975. P. 6–29 [Мячкин В.И., Костров Б.В., Соболев Г.А., Шамина О.Г. Основы физики очага и предвестники землетрясений // Физика очага землетрясения. М.: Наука. 1975. С. 6–29.].

Nadeau R.M., Dolenc D. Nonvolcanic tremors deep beneath the San Andreas Fault // Science. 2005. Vol. 307, No. 389. doi.org/10.1126/science.1107142.

Obara K., Hirose H. Non-volcanic deep low frequency tremors accompanying slow slips in the southwest Japan subduction zone // Tectonophysics. 2006. Vol. 417, No. 1–2. P. 33–51. doi.org/10.1016/j.tecto.2005.04.013.

Olami Z, Feder H.J.S, Christensen K. Self-organized criticality in a continuous, nonconservative cellular automaton modeling earthquakes // Physical Review Letters. 1992. Vol. 68. P. 1244–1247. doi.org/10.1103/PhysRevLett.68.1244.

Panteleev I., Plekhov O., Pankov I., Evseev A., Naimark O., Asanov V. Experimental investigation of the spatio-temporal localization of deformation and damage in sylvinite specimens under uniaxial tension // Engineering Fracture Mechanics. 2014. Vol. 129. P. 38–44. doi.org/10.1016/j.engfracmech.2014.08.004.

Peng Z., Gomberg J. An integrated perspective of the continuum between earthquakes and slow-slip phenomena // Nature Geoscience. 2010. Vol. 3, No. 9. P. 599–607. doi.org/10.1038/ngeo940.

Pushcharovsky Yu.M. Non-linear geodynamics (author's credo) // Geotectonics. 1993. Vol. 1. P. 3–7.

Rogers G., Dragert H. Episodic tremor and slip on the Cascadia subduction zone: The chatter of silent slip // Science. 2003. Vol. 300, No. 5627. P. 1942–1943. doi.org/10.1126/science.1084783.

Rosenau M., Lohrmann J., Oncken O. Shocks in a box: An analogue model of subduction earthquake cycles with application toseismotectonic forearc evolution // J. Geophys. Res. 2009. Vol. 114, No. B01409. doi.org/10.1029/2008JB005665.

Rosenau M., Corbi F., Dominguez S. Analogue earthquakes and seismic cycles: experimental modelling across timescales // Solid Earth. 2017. Vol. 8, 597–635. doi.org/10.5194/se-8-597-2017.

Sadovsky M.A., Balhovitinov L.G., Pisarenko V.F. Seismic processes in geophysical media // Izvestiya Physics of the Earth. 1982. Vol. 12. P. 3–18.

Sekine S., Hirose H., Obara K. Along-strike variations in short-term slow slip events in the southwest Japan subduction zone // Journal of Geophisical Research. 2010. Vol. 115. P. B00A27. doi.org/10.1029/2008JB006059.

Shelly D.R., Beroza G.C., Ide S. Non-volcanic tremor and low-frequency earthquake swarms // Nature. 2007. Vol. 446, No. 7133. P. 305–307. doi.org/10.1038/nature05666.

Seminsky K.Zh. Structural and Mechanical Properties of Clayey Pastes as Model Material in Tectonic Experiments. Institute of the Earth's Crust, Siberian Branch of the USSR Academy of Sciences, Irkutsk, 1986. 130 pp. VINITI 13.08.86. 5762–B86 [Семинский К.Ж. Структурно-механические свойства глинистых паст как модель- ного материала в тектонических экспериментах. Иркутск: ВИНИТИ, 1986. № 5762 (В 86). 130 с.].

Seminsky K.Zh. The Internal Structure of Continental Fault Zones. Tectonophysical Aspect. GEO, Novosibirsk, 2003. 244 pp. [Семинский К.Ж. Внутренняя структура континентальных разломных зон. Тектоно-физический аспект. Новосибирск: Изд-во СО РАН, филиал «ГЕО», 2003. 244 с.]

Seminsky K.Zh. Hierarchy of the zone-block structure of the lithosphere of Central and East Asia: the ratio between the size of fault zones and blocks at different levels of the hierarchy // Russian Geology and Geophysics. 2008. Vol. 49, No. 10. P. 1018–1030. doi.org/10.1016/j.rgg.2007.11.017.

Sherman S.I. Physical experiment in tectonics and the theory of similarity // Russian Geology and Geophysics. 1984. Vol. 3. P. 8–18. [Шерман С.И. Физический эксперимент в тектонике и теория подобия // Геология и геофизика. 1984. № 3. С. 8–18.]

Sherman S.I., Seminsky K.Zh., Bornyakov S.A., et al. Faulting in the Lithosphere. Shear Zones. Nauka, Novosibirsk, 1991. 261 pp. [Шерман С.И., Семинский К.Ж., Борняков С.А. и др. Разломообразование в литосфере: зоны сдвига. Новосибирск: Наука, 1991. 260 с.]

Sutton M.A., Orteu J.J., Schreier H.W. Image Correlation for Shape, Motion and Deformation Measurements: Basic Concepts, Theory and Applications. Springer, 2009. 316 pp.

Stoyanov S.S. Fault Zone Formation Mechanisms. Nedra, Moscow, 1977. 114 pp. [Стоянов

С.С. Механизм формирования разрывных зон. М.: Недра, 1977. 143 с.]

Tchalenko J.S. Similarities between shear zones of different magnitudes // Geological Society of America Bulletin. 1970. Vol. 81, No. 6. P. 1625–1640. doi.org/10.1130/0016-7606(1970)81[1625:SBSZOD]2.0.CO;2.

Tocher D. Earthquake energy and ground breakage // Bulletin of the Seismological Society of America. 1958. Vol. 48, No. 2. P. 147–153. doi.org/10.1785/ BSSA0480020147.

Turcotte D.L. Fractals and Chaos in Geology and Geophysics, Cambridge Univ. Press, Cambridge, U. K., 1997. 410 pp. doi.org/10.1017/CBO9781139174695.

Wei M., Kaneko Y., Liu Y., McGuire J.J. Episodic fault creep events in California controlled by shallow frictional heterogeneity // Nature Geoscience. 2013. Vol. 6, 1–5. doi.org/10.1038/ngeo1835.

Weijermars R., Schmeling H. Scaling of Newtonian and non-Newtonian fluid dynamics without inertia for quantitative modelling of rock flow due to gravity (including the concept of rheological similarity) // Phys. Earth Planet. Inter. 1986. Vol. 43, No. 4. P. 316–330. doi.org/10.1016/0031-9201(86)90021-X.

Wilcox R.E., Harding T.P., Seely D.R. Basic wrench tectonics // AAPG Bulletin. 1973. Vol. 57. P. 74–96.

Zubarev D.N., Morozov V.G., Repke G. Statistical mechanics of non-equilibrium processes. Fizmatlit, Moscow, 2002. 431 pp. [Зубарев Д.Н., Морозов В.Г., Репке Г. Статистическая механика неравновесных процессов. Физматлит, Москва, 2002. 431 с.]

Zhuo, Y. Q., Guo, Y. S., Ji, Y. T., et al. Slip synergism of planar strike-slip fault during metainstable state: Experimental research based on digital image correlation analysis // Science China Earth Sciences. 2013. Vol. 56. P. 1881–1887. doi.org/10.1007/s11430-013-4623-4.

Борняков Сергей Александрович,
кандидат геолого-минералогических наук,
664033 Иркутск, ул. Лермонтова, д. 128,
Институт земной коры СО РАН,
ведущий научный сотрудник,
email: bornyak@crust.irk.ru.
Bornyakov Sergey Alexandrovich,
candidate of geological and mineralogical sciences,
664033 Irkutsk, Lermontov str., 128,
Institute of the Earth's Crust SB RAS,
Leading Researcher,
email: bornyak@crust.irk.ru.

Го Яншуан,
доктор наук,
Институт геологии Китайского управления по землетрясениям, Пекин, Китай,
научный сотрудник,
email: guoysh@ies.ac.cn.
Guo Yanshuang,
Doctor of science,
Institute of Geology, China Earthquake Administration, Beijing, China,
Researcher,
email: guoysh@ies.ac.cn.

Пантелеев Иван Алексеевич,
кандидат геолого-минералогических наук,
Институт механики сплошных сред УрО РАН, Пермь, Россия,
старший научный сотрудник,
email: pia@icmm.ru.
Panteleev Ivan Alexeevich,
candidate of geological and mineralogical sciences,
Institute of Continuous Media Mechanics, Ural Branch of the Russian Academy of Sciences, Perm, Russia,
Senior Researcher,
email: pia@icmm.ru.

Жуо Ян-Цун,
доктор наук,
Институт геологии Сейсмологического бюро Китая, Пекин, Китай,
научный сотрудник,
email: zhuoyq@ies.ac.cn.
Zhuo Yan-Qun,
Doctor of science,
Institute of Geology, China Earthquake Administration, Beijing, China,
Researcher,
email: zhuoyq@ies.ac.cn.

Добрынина Анна Александровна,
кандидат геолого-минералогических наук,
664033 Иркутск, ул. Лермонтова, д. 128,
Институт земной коры СО РАН, Иркутск,
Ученый секретарь,
Геологический институт им. Н.Л. Добрецова СО РАН, Улан-Удэ,
тел.: 83952426900, 89501200270,
email: *scisecretary@crust.irk.ru.*
Dobrynina Anna Alexandrovna,

candidate of geological and mineralogical sciences,
664033 Irkutsk, Lermontov str., 128,
Institute of the Earth's Crust SB RAS,
Scientific secretary,
email: scisecretary@crust.irk.ru.

Саньков Владимир Анатольевич,
кандидат геолого-минералогических наук,
664033 Иркутск, ул. Лермонтова, д. 128,
Институт земной коры СО РАН, Иркутск,
заместитель директора по науке,
664003 Иркутск, ул. Ленина, д. 3,
Иркутский государственный университет, геологический факультет,
доцент,
email: sankov@crust.irk.ru.
Sankov Vladimir Anatolevich,
candidate of geological and mineralogical sciences,
664033 Irkutsk, Lermontov str., 128,
Institute of the Earth's Crust SB RAS,
Deputy Director for Science,
664003 Irkutsk, Lenin str., 3,
Irkutsk State University, Faculty of Geology,
Assystent Professor,
email: sankov@crust.irk.ru.

Салко Денис Владимирович,
664033 Иркутск, ул. Лермонтова, д. 128,
Институт земной коры СО РАН, Иркутск,
инженер,
email: salko@crust.irk.ru.
Salko Denis Vladimirovich,
664033 Irkutsk, Lermontov str., 128,
Institute of the Earth's Crust SB RAS,
Engineer,
email: salko@crust.irk.ru

Шагун Артем Николаевич,
кандидат геолого-минералогических наук,
664033 Иркутск, ул. Лермонтова, д. 128,
Институт земной коры СО РАН, Иркутск,
ведущий инженер,
email: shagun@crust.irk.ru.
Shagun Artem Nikolaevich,
candidate of geological and mineralogical sciences,
664033 Irkutsk, Lermontov str., 128,
Institute of the Earth's Crust SB RAS,
Lead Engineer,
email: shagun@crust.irk.ru.

Каримова Анастасия Алексеевна,
кандидат геолого-минералогических наук,
664033 Иркутск, ул. Лермонтова, д. 128,
Институт земной коры СО РАН, Иркутск,
младший научный сотрудник,
Иркутский государственный университет, Иркутск,
ст. преподаватель,
email: geowomen_nasty@mail.ru.
Karimova Anastasia Alekseevna,
candidate of geological and mineralogical sciences
664033 Irkutsk, Lermontov str., 128,
Institute of the Earth's Crust SB RAS,
Junior Researcher,
664003 Irkutsk, Lenin str., 3,
Irkutsk State University, Faculty of Geology,
Senior Lecturer,
email: geowomen_nasty@mail.ru.